J. Am. Chem. Soc. 1994, 116, 7369-7377

IR Flash Kinetic Spectroscopy of C—H Bond Activation of Cyclohexane-d_0 and -d_{12} by Cp*Rh(CO)$_2$ in Liquid Rare Gases: Kinetics, Thermodynamics, and an Unusual Isotope Effect

Richard H. Schultz, A. A. Bengali, M. J. Tauber, Bruce H. Weiller,[†] Eric P. Wasserman,[‡] K. R. Kyle,[§] C. Bradley Moore,* and Robert G. Bergman*

Contribution from the Department of Chemistry, University of California, Berkeley, California 94720, and Chemical Sciences Division, Lawrence Berkeley Laboratory, Berkeley, California 94720

Received March 31, 1994[⊗]

Abstract: Flash kinetic spectroscopy with infrared detection is used to probe C—H activation of cyclohexane-d_0 and -d_{12} by intermediates generated upon ultraviolet irradiation of Cp*Rh(CO)$_2$ (Cp* = $C_5(CH_3)_5$) in liquid rare gas (Rg = Kr or Xe) solution at low temperature (163–193 K). Upon UV photolysis, a new C—O stretching band (at 1946.5 cm^{-1} in Kr and at 1941.5 cm^{-1} in Xe) appears promptly, which we attribute to Cp*Rh(CO)(Rg). In the presence of hydrocarbon a second C—O stretching band (2002.5 cm^{-1} in Kr and 1998 cm^{-1} in Xe) grows in at the same observed rate as the disappearance of the 1946.5-cm^{-1} band. We attribute this second band to the alkyl hydride product, Cp*Rh(CO)(H)(C_6H_{11}). The concentration dependence of the observed reaction rate in Kr solution shows behavior consistent with a preequilibrium mechanism in which the initial Cp*Rh(CO)(Rg) complex equilibrates with a weakly bound Cp*Rh(CO)(alkane) complex (which has an IR carbonyl frequency unresolvable from that of the rare gas complex) followed by C—H activation of the latter. We observe a large normal kinetic isotope effect ($k_2^H/k_2^D \approx 10$) on the C—H activation step k_2, but, most unusually, a large *inverse* isotope effect on the preequilibrium constant ($K_{eq}^H/K_{eq}^D \approx 0.1$), implying that C_6D_{12} binds more strongly to the rhodium center than does C_6H_{12}. From the temperature dependence of k_2, we derive Eyring activation energies of 4.2 ± 0.5 kcal/mol for k_2^H and 5.3 ± 0.5 kcal/mol for k_2^D.

Introduction

In the decade since the first observation of the photolytic oxidative addition of alkane C—H bonds to group 9 transition metal centers (reaction 1, R = H, CH_3; L = CO, $P(CH_3)_3$; L′ = CO, H_2),[1,2] there has been considerable research effort devoted to understanding the reaction mechanism.[3–6]

$$\eta^5\text{-}C_5R_5MLL' + R'H \xrightarrow{h\nu} \eta^5\text{-}C_5R_5ML(R')(H) + L' \quad (1)$$

Two complications make such elucidation particularly difficult. The first problem is the exceptional reactivity of the photolytically produced intermediates. Although Cp*Ir(CO)$_2$ will activate alkanes in perfluoromethylcyclohexane,[2] even "inert" solvents such as fluorocarbons, SF_6, and SiF_4 undergo photolytic reaction with Cp*Ir(PMe$_3$)(H$_2$). This high reactivity of intermediate with solvent makes it difficult to systematically vary the concentration of organic reactant, thus rendering detailed kinetic studies difficult or impossible. A second challenge is the rapidity with which the intermediates activate the molecules they encounter, once again frustrating traditional kinetic studies.

To address the problem of high reactivity, we have chosen to perform our studies of transition metal-mediated alkane activation using liquefied rare gases (Kr and Xe) as solvents and the kinetic technique of flash photolysis. The use of liquid rare gases as substrates for organometallic photochemistry was first developed by Turner and co-workers[7] and has since been used by his group and others[5,8–10] to study a variety of otherwise intractable systems. Liquefied rare gases have several properties that make them appropriate solvents for the studies described herein. First, being monatomic, they are inert to chemical activation (although their interaction energies with transition metals can be on the order of 10 kcal/mol[11,12]). Another obvious advantage of liquid rare gases for kinetic techniques that rely on spectroscopic detection methods is their transparency to IR, visible, and UV light. In

---

[†] Present address: Mechanics and Materials Technology Center, The Aerospace Corporation, P.O. Box 92957, Los Angeles, CA 90009.

[‡] Present address: Union Carbide Chemicals and Plastics Corp., Bound Brook, NJ 08805.

[§] Present address: Mail Stop L-524, Lawrence Livermore National Laboratories, 7000 East Ave., Livermore, CA 94550.

[⊗] Abstract published in *Advance ACS Abstracts,* July 1, 1994.

(1) Janowicz, A. H.; Bergman, R. G. *J. Am. Chem. Soc.* **1982**, *104*, 352.

(2) Hoyano, J. K.; Graham, W. A. G. *J. Am. Chem. Soc.* **1982**, *104*, 3723.

(3) Janowicz, A. H.; Bergman, R. G. *J. Am. Chem. Soc.* **1983**, *105*, 3929. Bergman, R. G. *Science* **1984**, *223*, 902. Crabtree, R. H. *Chem. Rev.* **1985**, *85*, 245. Ephritikhine, M. *New J. Chem.* **1986**, *10*, 9. Nolan, S. P.; Hoff, C. D.; Stoutland, P. O.; Newman, L. J.; Buchanan, J. M.; Bergman, R. G.; Yang, G. K.; Peters, K. S. *J. Am. Chem. Soc.* **1987**, *109*, 3143.

(4) (a) Jones, W. D.; Feher, F. J. *J. Am. Chem. Soc.* **1984**, *106*, 1650. (b) Buchanan, J. M.; Stryker, J. M.; Bergman, R. G. *Ibid.* **1986**, *108*, 1537. (c) Periana, R. A.; Bergman, R. G. *Ibid.* **1986**, *108*, 7332.

(5) Weiller, B. H.; Wasserman, E. P.; Bergman, R. G.; Moore, C. B.; Pimentel, G. C. *J. Am. Chem. Soc.* **1989**, *111*, 8288.

(6) Wasserman, E. P.; Moore, C. B.; Bergman, R. G. *Science* **1992**, *255*, 315.

(7) (a) Maier, W. B., II; Poliakoff, M.; Simpson, M. B.; Turner, J. J. *J. Chem. Soc., Chem. Commun.* **1980**, 587. (b) Simpson, M. B.; Poliakoff, M.; Turner, J. J.; Maier, W. B., II; McLaughlin, J. G. *Ibid.* **1983**, 1355. (c) Upmacis, R. K.; Poliakoff, M.; Turner, J. J. *J. Am. Chem. Soc.* **1986**, *108*, 3645.

(8) Andrea, R. R.; Luyten, H.; Vuurman, M. A.; Stufkens, D. J.; Oskam, A. *Appl. Spectrosc.* **1986**, *40*, 1184. Howdle, S. M.; Poliakoff, M. *J. Chem. Soc., Chem. Commun.* **1989**, 1099.

(9) Sponsler, M. B.; Weiller, B. H.; Stoutland, P. O.; Bergman, R. G. *J. Am. Chem. Soc.* **1989**, *111*, 6891.

(10) (a) Jobling, M.; Howdle, S. M.; Healy, M. A.; Poliakoff, M. *J. Chem. Soc., Chem. Commun.* **1990**, 1287. (b) Perutz, R. N. *Pure Appl. Chem.* **1990**, *62*, 1103. (c) Drolet, D. P.; Lees, A. J. *J. Am. Chem. Soc.* **1992**, *114*, 4186.

(11) Turner, J. J.; Simpson, M. B.; Poliakoff, M.; Maier, W. *J. Am. Chem. Soc.* **1983**, *105*, 3898. Brown, C. E.; Ishikawa, Y.; Hackett, P. A.; Rayner, D. M. *Ibid.* **1990**, *112*, 2530.

(12) Weiller, B. H.; Wasserman, E. P.; Moore, C. B.; Bergman, R. G. *J. Am. Chem. Soc.* **1993**, *115*, 4326.

0002-7863/94/1516-7369$04.50/0

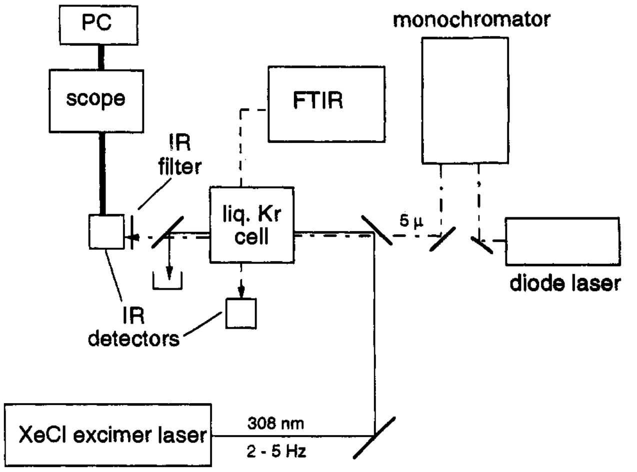

Figure 1. Instrumental schematic.

addition, their bulk properties such as viscosity and index of refraction are quite similar to those of liquid alkanes.[13]

In order to be able to fully follow the reaction over its entire course, we use flash kinetic infrared spectroscopy. Flash kinetic methods[14] have been used to study organometallic compounds (particularly transition metal carbonyl compounds) in solution in a variety of contexts, ranging from femtosecond and picosecond studies of solvation processes[15] to microsecond and millisecond studies of ligand substitution,[16] metal dimer photolysis,[17] intramolecular photochemistry,[18] and hydrosilation reactions.[19] As the probe of the intermediates and products, we use infrared absorption spectroscopy of the 5-μm C—O stretching region. Infrared spectroscopy as the means of detection has the immediate advantage that it gives detailed structural information about the species being probed. In addition, in the present case it has the additional advantage that transition metal carbonyl stretches are quite intense, making detection of the intermediates possible even in small concentrations.

Thus, the combination of noble gas solvents with IR flash kinetics has made it possible to perform a detailed kinetic and spectroscopic study of the temperature and concentration dependence of alkane activation by $Cp^*Rh(CO)_2$. Several years ago, we published a preliminary account of our work in this area, in which we examined the reaction of $Cp^*Rh(CO)_2$ with cyclohexane in liquid Kr.[5] Since that time, we have extended our research to include studies of reactions of perdeuterated cyclohexane in order to observe the H/D isotope effects in these reactions and the use of both Kr and Xe as solvents in order to better elucidate the effect of solvent on the kinetics. Finally, in our earlier report, we had used a CO laser as the infrared probe. Here, we use a continuously tunable lead salt diode laser in order to more fully resolve the time-dependent infrared spectrum.

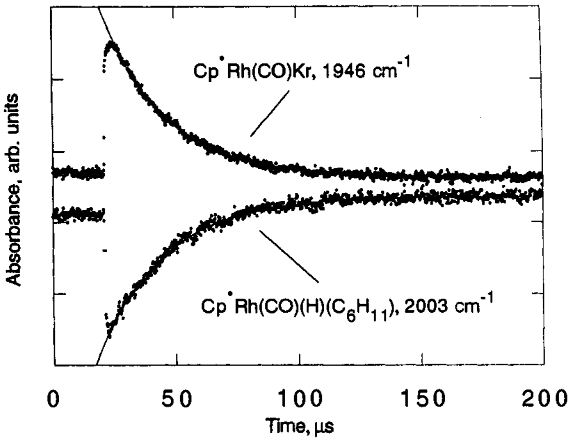

Figure 2. Typical transient traces. Shown are time-dependent absorbances at 1946 and 2003 cm^{-1} for photolysis of $Cp^*Rh(CO)_2$ in the presence of 3 mM C_6H_{12} in liquid Kr at −100 °C. Also shown are exponential fits to the data with k_{obs} = 38 000 s^{-1}.

Experimental Section

The experiments described in this report were performed on two versions of the flash kinetic spectrometer shown schematically in Figure 1. Reactions take place in a cell the design of which is based on those of Gadd and of Turner and co-workers.[20] The cell consists of a Cu block through which two perpendicular 1 cm diameter channels have been drilled (long axis 5 cm, short axis 1.43 cm) and capped with BaF_2 or CaF_2 windows. Reagents are admitted to the cell via a 1/8 in. diameter tube along the third axis. The cell is surrounded by a vacuum jacket to prevent condensation of atmospheric water on the cell windows. The temperature is measured by a Cu-constantan thermocouple and kept stable to ±1 °C by an Omega model CN2002-T temperature controller that directs resistive heating of two 50-Ω resistors attached to the Cu block and a flow of liquid N_2 through a channel in the Cu block. The temperature control apparatus was calibrated with a series of slush baths.

Reaction is initiated by a 308-nm UV pulse from a XeCl excimer laser (Lambda-Physik model EMG-103 run at 2–10 Hz, pulse fwhm ca. 20 ns, output 60–90 mJ/pulse), which passes down the long axis of the cell. In order to minimize artifacts caused by uneven illumination of the sample by the photolysis pulse, the UV beam is not focused. Thus, at the cell, the UV beam diameter is >10 cm, so that the photolysis light fills the cell completely; the UV energy entering the cell is approximately 5 mJ/pulse. The infrared probe beam traverses the cell colinear to and centered within the UV beam, and a beam dump is inserted after the cell to prevent UV radiation from impinging on the IR detector. The time-dependent signal is then passed to a digitizer, and 16–200 shots are averaged, followed by collection of an equal number of background traces collected with the UV signal blocked. The resulting transient (foreground minus background) is then saved on a computer. The initial configuration of the instrument, with a home-built CO laser as IR source, liquid-He-cooled Ge:Cu detector, and Tektronix model 7912 digitizer, has been described in detail previously.[21] For more recent experimental runs, the system was reconfigured. Currently, the IR source is a tunable PbSSe diode laser (Mütek model MDS 2020) which lases from 1896–2070 cm^{-1} and has a maximum single-mode output of ≈1 mW. The output is collimated to a 4–5 mm diameter beam and passed through a monochromator (Spex model 270M, 0.25 m, grating blazed at 4 μm, nominal resolution 0.2 cm^{-1} at 5 μm) before passing through the cell. A liquid-N_2-cooled InSb detector (Cincinnati Electronics model SDD-32E0-S1-05M, 2-mm diameter, 70-ns rise time) is used for IR detection. In order to be able to turn the raw transient signal into relative absorbance, we first obtain a normalization signal by chopping the diode laser output at 485 Hz and then measuring the signal intensity after the light has passed through the cell. Data

---

(13) Cogwill, D. F.; Norberg, R. E. *Phys. Rev. B* **1976**, *13*, 2773. Chen, S. H.; Davis, H. T. *J. Chem. Phys.* **1981**, *75*, 1422. Sinnock, A. C. *J. Phys. C.* **1980**, *13*, 2375.

(14) Porter, G. *Proc. R. Soc.* (*London*) **1950**, *A200*, 284. Christie, M. I.; Norrish, R. G. W.; Porter, G. *Ibid.* **1952**, *A216*, 152.

(15) Simon, J. D.; Peters, K. S. *Chem. Phys. Lett.* **1983**, *98*, 53. Wang, L.; Zhu, X.; Spears, K. G. *J. Am. Chem. Soc.* **1988**, *110*, 8695; *J. Phys. Chem.* **1989**, *93*, 2. Lee, M.; Harris, C. B. *J. Am. Chem. Soc.* **1989**, *111*, 8963. Joly, A. G.; Nelson, K. F. *J. Phys. Chem.* **1989**, *93*, 2876; *Chem. Phys.* **1991**, *152*, 69. Anfinrud, P. A.; Han, C.-H.; Lian, T.; Hochstrasser, R. M. *J. Phys. Chem.* **1991**, *95*, 574. Dougherty, T. P.; Heilweil, E. J. *J. Chem. Phys.* **1994**, *100*, 4006.

(16) See, for example: (a) Lees, A. J.; Adamson, A. W. *Inorg. Chem.* **1981**, *20*, 4381. (b) Kelly, J. M.; Long, C.; Bonneau, R. *J. Phys. Chem.* **1983**, *87*, 3344. (c) Church, S. P.; Grevels, F. W.; Hermann, H.; Schaffner, K. *Inorg. Chem.* **1984**, *23*, 3830; **1985**, *24*, 418. (d) Church, S. P.; Grevels, F.-W.; Hermann, H.; Kelly, J. M.; Klotzbücher, W. E.; Schaffner, K. *J. Chem. Soc., Chem. Commun.* **1985**, 594. (e) Zhang, S.; Dobson, G. R. *Polyhedron* **1990**, *9*, 2511. (f) Dixon, A. J.; George, M. W.; Hughes, C.; Poliakoff, M.; Turner, J. J. *J. Am. Chem. Soc.* **1992**, *114*, 1719.

(17) McKee, S. D.; Bursten, B. E. *J. Am. Chem. Soc.* **1991**, *113*, 1210. Dixon, A. J.; George, M. W.; Hughes, C.; Poliakoff, M.; Turner, J. J. *Ibid.* **1992**, *114*, 1719. Knorr, J. R.; Brown, T. L. *Ibid.* **1993**, *115*, 4087. Yao, Q.; Bakac, A.; Espenson, J. H. *Organometallics* **1993**, *12*, 2010.

(18) Belt, S. T.; Ryba, D. W.; Ford, P. C. *J. Am. Chem. Soc.* **1991**, *113*, 9524. Bal Reddy, K.; Hoffmann, R.; Konya, G.; van Eldik, R.; Eyring, E. M. *Organometallics* **1992**, *11*, 2319.

(19) Zhang, S.; Dobson, G. R.; Brown, T. L. *J. Am. Chem. Soc.* **1991**, *113*, 6908.

(20) (a) Wasserman, E. P. Ph.D. Thesis, University of California, Berkeley, CA, 1989. (b) Maier, W. B., II.; Poliakoff, M.; Simpson, M. B.; Turner, J. J. *J. Mol. Struct.* **1982**, *80*, 83.

(21) Wasserman, E. P.; Moore, C. B.; Bergman, R. G. *J. Am. Chem. Soc.* **1988**, *110*, 6076.

collection is performed by a LeCroy model 9310 300-MHz digital oscilloscope controlled by an IBM-PC (80486) clone using a Turbo Pascal program. Typical experimental traces are shown, along with least-squares single-exponential fits to the data, in Figure 2.

To prepare the photolysis solutions, first, a stock solution of Cp*Rh(CO)$_2$ (generally 1–2 mM) in hexane or cyclohexane is prepared. An aliquot (0.2–1 mL) of this solution is then injected into the cell and the solvent removed. The rare gas is flowed through a stainless steel line containing cyclohexane vapor and into the cell, which is pressurized to 50–100 psi at room temperature. The cell is then cooled (generally to about −140 °C for Kr and to about −90 °C for Xe), reopened to the line to fill the cell with liquid rare gas, and warmed to the temperature at which the experiment is to be performed. The cell pressure generally is kept between 100 and 600 psi during the course of an experiment. A small magnetic stirrer ensures that the solution is well-mixed. For a given concentration of cyclohexane, photolysis experiments are then carried out at several temperatures, after which the rare gas/cyclohexane solution is transferred into an evacuated stainless steel U-tube. The cell is then warmed back to room temperature, vented with Ar, and rinsed several times with hexanes before another aliquot of stock solution is added. Complete disassembly and cleaning of the cell and windows is done approximately once weekly.

Reagent concentrations are estimated by integrating the infrared absorbances measured *in situ* using a commercial FTIR instrument with the beam passing through the short axis of the cell (either a Perkin-Elmer 1750 (2-cm^{-1} resolution, DTGS detector), Nicolet 510 (2-cm^{-1} resolution, MCT detector), or Nicolet 550 (0.5-cm^{-1} resolution, MCT detector). For the hydrocarbon reagents, gas-phase integrated band strengths are taken from the literature[22] and corrected for the index of refraction of the rare gas solvent.[23] At high concentrations of C_6D_{12}, a weak overtone at approximately 1998 cm^{-1} was used for concentration estimation, its integrated band strength having been determined from comparison of its intensity with those of the bands whose values were reported in the literature.[22] We independently verified that the FTIR response is linear at all alkane concentrations used by making stock solutions of cyclohexane in CCl_4 and verifying that the integrated absorbances remain linear with concentration over the range of absorbance we measure in the actual high-pressure cell. The concentration of Cp*Rh(CO)$_2$ was determined by comparing the integrated band strengths of its C—O absorbances in rare gas solution with those in the stock solution and correcting for relative indices of refraction and cell path length. In all cases, the concentration of Cp*Rh(CO)$_2$ in rare gas was approximately 10^{-5} M, which is sufficiently dilute to assure that all of the experiments were performed under pseudo-first-order conditions and that ≈90% of the incident UV passes through the cell.

Cp*Rh(CO)$_2$ was either synthesized by a literature procedure[24] and purified by sublimation or obtained from Strem and used without further purification. C_6H_{12} was obtained from Fisher and distilled over CaH_2. C_6D_{12} (99.7 atom % D) was obtained from Cambridge Isotopes and used without further purification. Kr and Xe (both 99.999%) were obtained from Spectra Gases. Lot analyses provided with each tank showed that non-rare-gas impurities such as N_2, O_2 and H_2O were at or below the parts per million level.

Results

1. Photolysis of Cp*Rh(CO)$_2$ in Liquid Kr (No Added Alkane). When Cp*Rh(CO)$_2$ is photolyzed in the absence of any other reactants, depletion of the parent occurs, as indicated by a decrease in the solution's absorbance at the Cp*Rh(CO)$_2$ carbonyl stretching frequencies coincident with the laser flash. A transient absorption appears at 1946.5 cm^{-1} within the risetime of the detector having a half-life on the order of 1 ms. We attribute this absorption to the C—O stretching frequency of the solvated monocarbonyl intermediate Cp*Rh(CO)(Kr), which is presumably formed within picoseconds of the loss of the carbonyl ligand.[15] We base this assignment on our failure to observe any other absorbances in the carbonyl region and the observation that in the presence of CO the disappearance of the absorbance at 1946.5 cm^{-1} and the reappearance of the parent Cp*Rh(CO)$_2$ carbonyl stretches occur at the same observed rate. Although the disappearance of Cp*Rh(CO)Kr was not accompanied by any observable product growth, the rate is consistent with a nearly diffusion-limited reaction with unphotolyzed parent to form Cp*$_2$Rh$_2$(CO)$_3$.

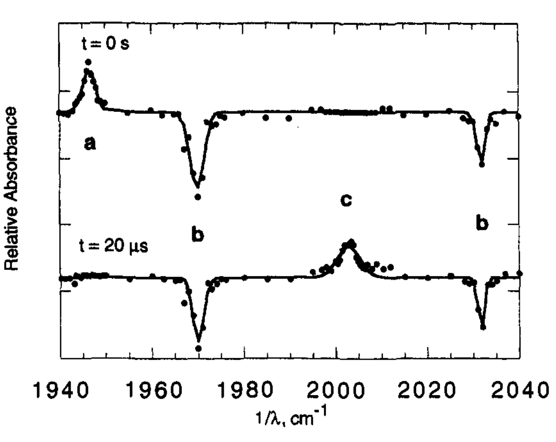

Figure 3. Time-dependent infrared spectrum of the photolysis of Cp*Rh(CO)$_2$ in Kr in the presence of 0.01 M C_6H_{12} at −90 °C. Shown are the relative absorbances ≈0.5 and 20 μs after the photolysis pulse, normalized to the Cp*Rh(CO)$_2$ concentration at the time each wavelength data point was collected. The peak marked **a** corresponds to Cp*Rh(CO)Kr; the negative peaks marked **b** correspond to the disappearance of parent Cp*Rh(CO)$_2$; and the peak marked **c** corresponds to the product, Cp*Rh(CO)(H)(C_6H_{11}).

2. Photolysis of Cp*Rh(CO)$_2$ in Kr in the Presence of C_6H_{12}. When photolysis is performed in the presence of C_6H_{12}, disappearance of the absorption at 1946.5 cm^{-1} (attributed in this case to a mixture of Cp*Rh(CO)(Kr) and Cp*Rh(CO)(C_6H_{12}) as detailed below) is accompanied by the growth of a new absorbance at 2002.5 cm^{-1} that arises with the same observed rate (see Figure 2). A time-dependent IR spectrum, collected by monitoring the time-dependent absorption between 1920 and 2040 cm^{-1}, is shown in Figure 3. We assign this new band to the C–H activated complex, Cp*Rh(CO)(H)(C_6H_{11}). This assignment is based on several considerations. First, the increase in CO stretching frequency implies formal oxidation of the Rh center, consistent with the known CO absorbances of several previously characterized molecules of the form Cp*Rh(CO)RR′.[25] Furthermore, our observed peak at 2002.5 cm^{-1} is consistent with those observed for Rh alkyl hydrides in low-temperature matrices[26] and in alkane solution.[27] Finally, although it is not possible to observe a stable CH-activated product (which has been described by Belt *et al.*[27] as being "exceptionally unstable with respect to formation of other products via reductive elimination of alkane") via FTIR under the conditions of our experiment, it is possible to observe an IR absorbance at approximately 2003 cm^{-1} that has a lifetime of several minutes in liquid Kr solution by exposing the solution either to the output of a CW Hg arc lamp with a quartz filter[20] or to several hundred excimer laser shots with the stirrer turned off. Even in this case, we were not able to observe any IR bands corresponding to a Rh–H stretch, presumably because this band is too weak at the concentrations of Cp*Rh(CO)(H)(C_6H_{11}) present in our experiment; similarly, Rest *et al.*[26] failed to observe the analogous band in their matrix study.

One other peculiarity of the observed product growth requires comment. As seen in Figure 2, the product growth at 2002.5 cm^{-1} occurs following a *decrease* in absorbance within the detector risetime. The most likely explanation for this behavior is that the alkyl hydride product is itself photolabile, either producing the Cp*Rh(CO)Kr intermediate and C_6H_{12} or losing CO to form Cp*Rh(H)(C_6H_{11})Kr (the latter species being invisible to our apparatus as it does not contain any carbonyl ligands). Thus, at the flash, some amount of the alkyl hydride already present from

---

[22] Hogan, T. R.; Steele, D. *J. Mol. Struct.* **1986**, *141*, 315.

[23] Sinnock, A. C. *J. Phys. C: Solid State Phys.* **1980**, *13*, 2375.

[24] Kang, J. W.; Maitlis, P. M. *J. Organomet. Chem.* **1971**, *26*, 393.

[25] Hill, R.; Knox, A. R. *J. Chem. Soc., Dalton Trans.* **1975**, 2622.

[26] Rest, A. J.; Whitwell, I.; Graham, W. A. G.; Hoyano, J. K.; McMaster, A. D. *J. Chem. Soc., Dalton Trans.* **1987**, 1181.

[27] Belt, S. T.; Grevels, F.-W.; Klotzbücher, W. E.; McCamley, A.; Perutz, R. N. *J. Am. Chem. Soc.* **1989**, *111*, 8373.

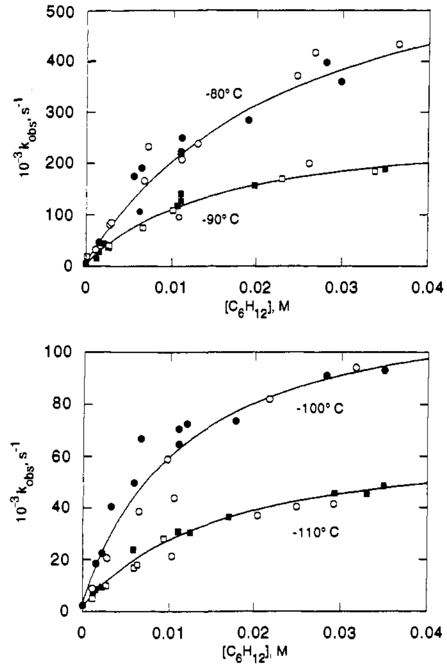

Figure 4. Observed pseudo-first-order rate constants for activation of C_6H_{12} by $Cp^*Rh(CO)_2$ divided by 1000 as a function of $[C_6H_{12}]$ at various temperatures (averages of intermediate decay rate and product growth rate). Open symbols are for data collected using a CO laser as the infrared probe, and solid symbols for data collected using a diode laser as the infrared probe. The solid lines represents fits to the data using the kinetic model discussed in the text.

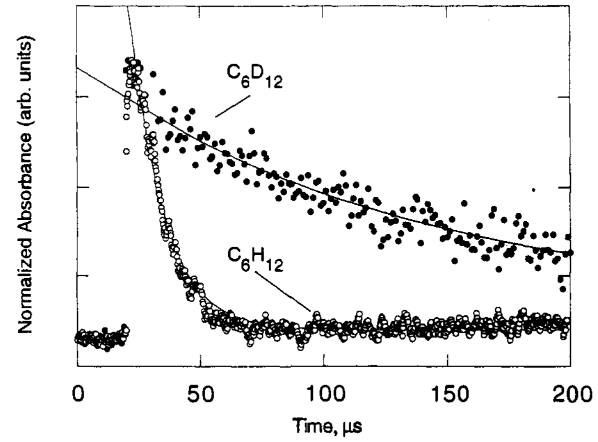

Figure 5. A comparison of the transient absorption at 1946.5 cm^{-1} for activation of C_6H_{12} and C_6D_{12} in Kr. Both transients were taken at −100 °C and 0.012 M alkane. The solid lines are exponential fits to the transient ($k_{obs}(C_6H_{12}) = 7.6 \times 10^4$ s^{-1}; $k_{obs}(C_6D_{12}) = 7.5 \times 10^3$ s^{-1}).

previous flashes dissociates, causing a decrease in absorption from the preflash baseline. Further evidence for this explanation is that if product growth is monitored starting with the very first UV flash, it rises from the baseline, and it is only after several dozen excimer laser flashes that the initial decrease is observed.

The concentration and temperature dependences of the observed reaction rates are shown in Figure 4. Clearly, the observed concentration dependence deviates from simple first-order behavior in $[C_6H_{12}]$ at all temperatures and shows pronounced curvature to reach a limiting rate at higher alkane concentrations. The mechanistic implications of this observed saturation behavior are discussed below.

3. Photolysis of $Cp^*Rh(CO)_2$ in Kr in the Presence of C_6D_{12}. When C_6D_{12} (perdeuteriocyclohexane) is used as the alkane, once again a transient absorbance is observed at 1946.5 cm^{-1} and product growth at 2002.5 cm^{-1}.[28] The kinetic behavior, however, shows two dramatic differences relative to that of C_6H_{12}. First,

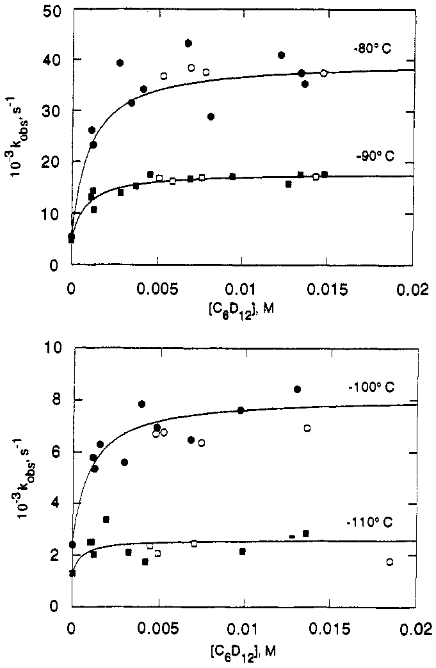

Figure 6. Observed pseudo-first-order rate constants for activation of C_6D_{12} by $Cp^*Rh(CO)_2$ divided by 1000 as a function of $[C_6D_{12}]$ at various temperatures (averages of intermediate decay rate and product growth rate at low concentration, intermediate decay rate only at high concentration[28]). Open symbols are for data collected using a CO laser as the infrared probe, and closed symbols for data collected using a diode laser as the infrared probe. The solid lines represent fits to the data using the kinetic model discussed in the text.

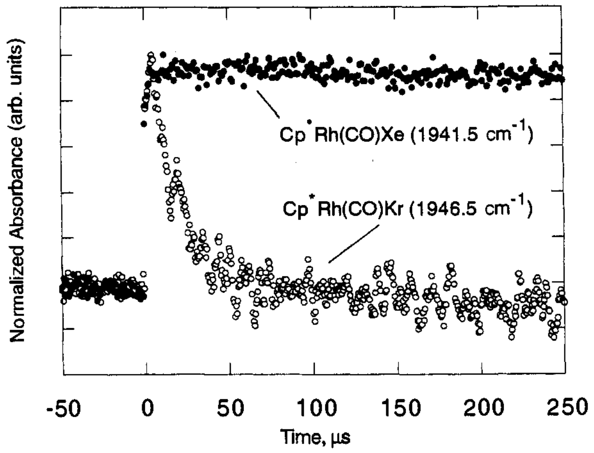

Figure 7. Transient infrared absorbances observed upon photolysis of $Cp^*Rh(CO)_2$ in the presence of 0.002 M C_6H_{12} in liquid Kr (1946.5 cm^{-1}, open circles) and liquid Xe (1941.5 cm^{-1}, solid circles) at −80 °C.

the observed reaction rate is approximately 1 order of magnitude slower with C_6D_{12} than it is with C_6H_{12}, as exemplified by the traces shown in Figure 5. In addition, with C_6D_{12} there is essentially *no* concentration dependence of the observed rate (Figure 6). That is, even at the lowest C_6D_{12} concentration used (<0.001 M), the observed rate appears to have already nearly reached its limiting value. The significance of these two striking observations is discussed in detail below.

4. Photolysis in Liquid Xe. In order to probe the effects of the solvent on the observed rate and provide an additional test of our hypotheses about the mechanism discussed below, we performed a series of experiments using liquid Xe as the solvent.

---

[28] At high C_6D_{12} concentrations, it was not always possible to make an accurate independent measurement of the product growth because of interference from a C_6D_{12} infrared band centered at 1998 cm^{-1}. In these cases, we only report the rate for disappearance of the intermediate, but the product growth could always be fit to the same observed rate even when the data were too noisy to fit *a priori*.

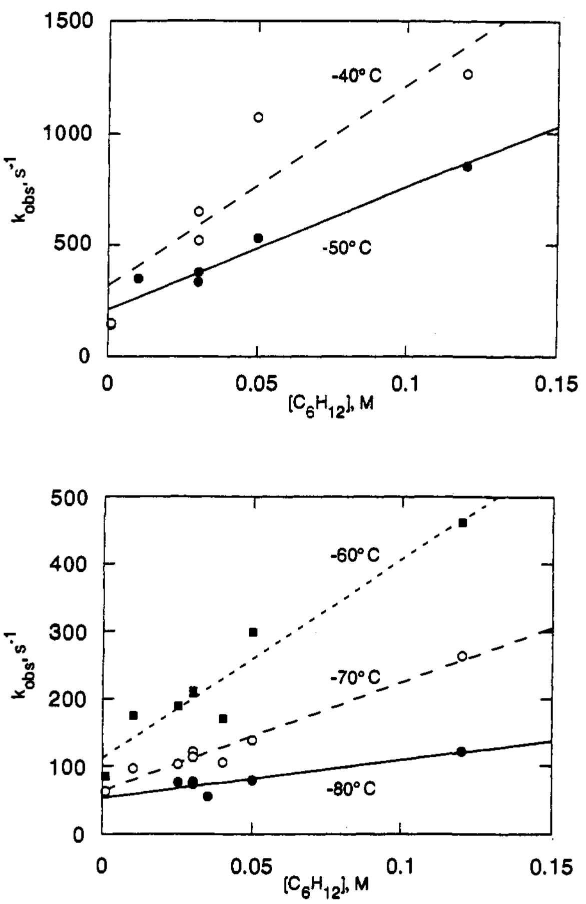

Figure 8. Observed pseudo-first-order rate constant plotted as a function of temperature and concentration for the activation of C_6H_{12} by $Cp^*Rh(CO)_2$ in liquid Xe with linear fits to k_{obs} as a function of $[C_6H_{12}]$.

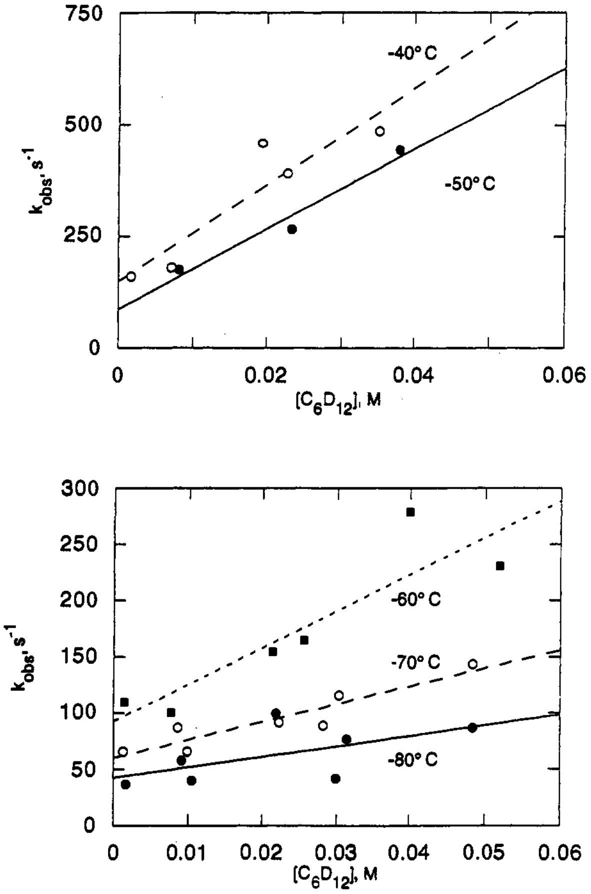

Figure 9. Observed pseudo-first-order rate constant plotted as a function of temperature and concentration for the activation of C_6D_{12} by $Cp^*Rh(CO)_2$ in liquid Xe with linear fits to k_{obs} as a function of $[C_6D_{12}]$.

In this medium, the observed rates are on the order of 100 times slower than they are in liquid Kr, even at temperatures 100 °C higher.[29] Figure 7 illustrates this dramatic difference. In our study of the reaction of Cp*Rh(CO)Xe with CO,[12] we also observed a diminution of the rate by a factor of approximately 100 relative to that of Cp*Rh(CO)Kr. The concentration and temperature dependences of the rates for the present results are shown in Figure 8 for C_6H_{12} and in Figure 9 for C_6D_{12}. The qualitative difference in the concentration dependence of the observed rate from that in liquid Kr is also striking. No deviation from linearity is observed in the concentration dependence of the observed rate in liquid Xe, even though the maximum concentration at which experiments were done is much higher than the concentrations at which curvature becomes apparent in Figures 4 and 6. Furthermore, unlike the reactions in liquid Kr, there is no significant isotope effect on the observed rate in liquid Xe. The implications of these observations are discussed in detail below.

Discussion

1. Photolysis in Kr: Determining the Reaction Mechanism. We believe that the most reasonable explanation for the observed behavior of k_{obs} (the observed rate for disappearance of intermediate and appearance of product) as a function of alkane concentration in liquid Kr is that shown in Scheme 1.[5,27] Upon photolysis, the parent $Cp^*Rh(CO)_2$ loses a carbonyl ligand to form the solvated species I. In room-temperature alkane solutions of metal carbonyl compounds, such solvation has been observed to occur in picoseconds.[15,30] This solvated species then quickly achieves an equilibrium with a weakly bound metal–alkane species **II**, which is presumably a "σ-complex" in which the metal atom interacts with, but has not yet activated, an alkane C—H bond. This species then undergoes intramolecular activation of the alkane at a rate k_2 to form the final alkyl hydride product. For completeness, we include all other processes that remove I as described in the Results section, with a pseudo-first-order rate of k_3. This scheme predicts that the observed rate as a function

Scheme 1

$$Cp^*Rh(CO)_2 \xrightarrow[\text{liq Kr}]{h\nu} \underset{\textbf{I}}{Cp^*Rh(CO)\cdots Kr} + CO$$

$$\textbf{I} + C_6H_{12} \overset{K_{eq}}{\rightleftarrows} \underset{\textbf{II}}{Cp^*Rh(CO)\cdots C_6H_{12}} + Kr$$

$$\textbf{II} \xrightarrow{k_2} \underset{\textbf{III}}{Cp^*Rh(CO)(C_6H_{11})(H)}$$

$$\textbf{I} \xrightarrow{k_3} \text{products}$$

---

[29] Indeed, at low cyclohexane concentration, the rates are slow enough to become distorted by the ca. 40 Hz low-frequency bandpass of the digital oscilloscope. To ensure that we were measuring an actual transient rather than the response of the oscilloscope, we ran a series of experiments first with the scope AC coupled and then with the scope DC coupled and a 12-μF capacitor in series with the output. The observed decays measured in these two ways differed only by the AC time constant of the oscilloscope. In general, it was not practical to run the scope DC coupled without the capacitor because the detector output DC offset of 0.2 V is 5–10 times larger than typical transient signal maxima.

[30] Although we adopt for convenience the notation "Cp*Rh(CO)···Kr" to describe the solvated species I, we make no specific claims about its actual structure or stoichiometry.

Table 1. Fitting Parameters (Eq 2) for Activation of C_6H_{12} in Liquid Kr

T (K)	k_2 (s^{-1})	K_{eq}	k_3 (s^{-1})
	C_6H_{12}		
193	$(7.02 \pm 0.84) \times 10^5$	$(9.09 \pm 2.03) \times 10^2$	7.8×10^3
183	$(2.79 \pm 0.26) \times 10^5$	$(1.46 \pm 0.31) \times 10^3$	4.7×10^3
173	$(1.24 \pm 0.12) \times 10^5$	$(2.05 \pm 0.50) \times 10^3$	3.1×10^3
163	$(6.85 \pm 0.62) \times 10^4$	$(1.45 \pm 0.27) \times 10^3$	1.9×10^3
	C_6D_{12}		
193	$(3.98 \pm 0.29) \times 10^4$	$(2.27 \pm 1.19) \times 10^4$	5.4×10^3
183	$(1.80 \pm 0.08) \times 10^4$	$(2.76 \pm 0.87) \times 10^4$	4.8×10^3
173	$(8.11 \pm 0.3) \times 10^3$	$(2.37 \pm 1.0) \times 10^4$	2.5×10^3
163	$(2.6 \pm 0.3) \times 10^3$	$(4.50 \pm 2) \times 10^4$	1.3×10^3

of alkane concentration should be given by eq 2.

$$k_{obs} = \frac{k_2[C_6H_{12}]}{[C_6H_{12}] + [Kr]/K_{eq}} + \frac{k_3}{1 + (K_{eq}[C_6H_{12}]/[Kr])} \tag{2}$$

Scheme 1 thus predicts that, at concentrations of C_6H_{12} where $[C_6H_{12}] \gg [Kr]/K_{eq}$, k_{obs} should saturate at k_2 if the second term is negligible. As $k_2[C_6H_{12}] \gg k_3[Kr]/K_{eq}$ for all systems studied here (Table 1) this condition is fulfilled. Thus, by fitting k_{obs} as a function of alkane concentration to eq 2 (using literature values[31] for the density of liquid Kr), we derive the values of k_2, k_3, and K_{eq} presented in Table 1;[32] the relevant fits are shown graphically in Figures 4 and 6. Because the saturation rate constant is that associated with the intramolecular activation step, its value should depend on the nature of the alkane, as is actually observed.

Although this scheme postulates two different intermediates, I and II, we observe transient absorbance at only one C—O stretching frequency. We therefore must assume that the C—O stretches of I and II overlap to a sufficient extent as to be indistinguishable by our instrument.[33] Additionally, we cannot absolutely eliminate the somewhat more complicated rate law derived by making the steady-state assumption for II (i.e. $d[\mathbf{II}]/dt \approx 0$) rather than the preequilibrium assumption (i.e. $k_{-1}[Kr] \gg k_2$). This rate law is similar to that given by eq 2, including a rise to saturation at $k_{obs} = k_2$, except that the term $[Kr]/K_{eq}$ ($=k_{-1}[Kr]/k_1$) of eq 2 becomes $(k_{-1}[Kr] + k_2)/k_1$. Attempts to model the concentration dependence of the observed rate by using the exact analytical solution to the rate equations[34] were most successful when $k_{-1}[Kr] \gg k_2$ (i.e. when the preequilibrium assumption is valid), but in any case, the steady-state mechanism would in the worst case make our reported values for K_{eq} high by a factor of 2. Furthermore, such a scheme would not affect our reported measurements of k_2 and does not change the qualitative conclusions about the isotope effects on the conversion of I to II detailed below.

There is additional evidence both for the mechanism proposed in Scheme 1 and against other mechanisms that might yield similar kinetics. Ligand substitution reactions at metal centers with η^5 ligands (Cp, Cp*, indenyl, etc.) have long been presumed to go through associative mechanisms.[35,36] In the commonly accepted picture, the reaction proceeds through an intermediate in which the η^5 ligand "slips" to an η^3 configuration, which allows the incoming ligand to bond to the metal center while still leaving it as an 18-electron species. It is reasonable to assume that the monocarbonyl solvate species I will react in a similar manner. In other kinetic studies of systems more directly revelant to the present one (room-temperature flash kinetic studies on reactions of $CpRh(CO)_2$ ($Cp = C_5H_5$) performed by Belt *et al.*[27] and on $CpRh(CO)_2$ and $Cp^*Rh(CO)_2$ performed by Drolet and Lees[37] and our low-temperature study[12] of the reaction of $Cp^*Rh(CO)(Xe)$ with CO), it was concluded that the reaction proceeds by an associative mechanism in which the incoming ligand attacks the solvated monocarbonyl intermediate. It seems reasonable that species I would behave kinetically like these analogous monocarbonyl intermediates. Scheme 1 also correctly predicts the strong isotope effect on k_2 shown pictorially in Figure 5, tabulated in Table 1, and discussed in more detail below. Finally, we expect the truly unsolvated gas-phase CpRh(CO) species reacts at the gas-diffusion-controlled rate with a wide range of molecules.[6] Because in the condensed-phase system studied here, observed rates are significantly slower than diffusion-limited, a solvated species lower in energy than the "naked" monocarbonyl must be involved.

Scheme 1 posits as intermediates metal–rare gas and metal–alkane complexes. There is significant experimental and theoretical precedent for such species. $Cr(CO)_5Xe$ was first observed by FTIR in liquid Kr solution by Simpson *et al.* in 1983,[7b] and since then, other transition metal–rare gas complexes have been observed in both gas[11,38] and condensed[39] phases. As mentioned above, these complexes tend to be bound by 5–10 kcal/mol,[11,39] and hence it is reasonable to invoke them in our system. Evidence for "σ-bound" alkane complexes such as II in which the metal center interacts with the σ-electrons of the alkane C—H bond, while less direct, is significant. Buchanan *et al.*[4b] attributed the deuterium scrambling patterns they observed in activation of isotopically labeled cyclohexane by $Cp^*Ir(P(CH_3)_3)(H_2)$ to a σ-complex intermediate in which the metal center interacts with one or possibly two C–H bonds. Similarly, Periana and Bergman[4c] found that postulating the existence of a σ-complex would best explain their observations of rearrangements of $Cp^*(PCH_3)_3Rh(H)(alkyl)$ complexes. In addition, Bullock *et al.*[40] have invoked a σ-complex $Cp_2W(CH_4)$ and Gould and Heinekey[41] a σ-complex $Cp_2Re(CH_4)X$ ($X = Cl^-$ or BF_4^-) to explain scrambling in the analogous methyl hydrides. Neutral[11,42] and ionic[43] transition metal–alkane complexes have also been observed in the gas phase. Several theoretical studies of alkane C—H bond activation have indicated as well that a metal–alkane complex can exist as a local minimum on the potential energy surface.[44]

---

[31] Streett, W. B.; Stavely, L. A. K. *J. Chem. Phys.* **1971**, *55*, 2495.

[32] In our initial report on this system[5] we did not explicitly consider reactions other than C–H activation that remove the intermediate from the system.

[33] Recent studies of the reaction of $Cp^*Rh(CO)_2$ with neopentane-d_{12} (Bengali, A. A.; Schultz, R. H.; Bergman, R. G.; Moore, C. B. *J. Am. Chem. Soc.*, submitted for publication) show that, in that system, IR bands arising from intermediates analogous to both I and II can be resolved, but their C—O stretching frequencies are separated by less than 1 cm^{-1}.

[34] The differential equations can be solved exactly by using Laplace transforms; the resulting solutions, however, are quite unwieldy. See: Espenson, J. H. *Chemical Kinetics and Reaction Mechanisms*; McGraw-Hill: New York, 1981; Chapter 4, and references therein.

[35] Hart-Davis, A. J.; Mawby, R. J. *J. Chem. Soc. A* **1969**, 2403. Hart-Davis, A. J.; White, C.; Mawby, R. J. *Inorg. Chim. Acta* **1970**, *4*, 441. Caddy, P.; Green, M.; O'Brien, E.; Smart, L. E.; Woodward, P. *Angew. Chem., Int. Ed. Engl.* **1977**, *16*, 648.

[36] Rerek, M. E.; Basolo, F. *Organometallics* **1983**, *2*, 372. Casey, C. P.; O'Connor, J. M.; Jones, W. D.; Haller, K. J. *Ibid.* **1983**, *2*, 535. Ji, L.-N.; Rerek, M. E.; Basolo, F. *Ibid.* **1984**, *3*, 740. O'Connor, J. M.; Casey, C. P. *Chem. Rev.* **1987**, *87*, 307. Casey, C. P.; Widenhofer, R. A.; O'Connor, J. M. *J. Organomet. Chem.* **1992**, *428*, 99. Bartz, J. A.; Barnhart, T. M.; Galloway, D .B.; Huey, L. G.; Glenewinkel-Meyer, T.; McMahon, R. J.; Crim, F. F. *J. Am. Chem. Soc.* **1993**, *115*, 8389.

[37] Drolet, D. P.; Lees, A. J. *J. Am. Chem. Soc.* **1990**, *112*, 5878; **1992**, *114*, 4186.

[38] Wells, J. R.; Weitz, E. *J. Am. Chem. Soc.* **1992**, *114*, 2783.

[39] Weiller, B. H. *J. Am. Chem. Soc.* **1992**, *114*, 10910.

[40] Bullock, R. M.; Headford, C. E. L.; Hennessy, K. M.; Kegley, S. E.; Norton, J. R. *J. Am. Chem. Soc.* **1989**, *111*, 3897.

[41] Gould, G. L.; Heinekey, D. M. *J. Am. Chem. Soc.* **1989**, *111*, 5502.

[42] Ishikawa, Y.; Brown, C. E.; Hackett, P. A.; Rayner, D. M. *Chem. Phys. Lett.* **1988**, *150*, 506. Caroll, J. J.; Weisshaar, J. C. *J. Am. Chem. Soc.* **1993**, *115*, 800.

[43] (a) Tonkyn, R.; Ronan, M.; Weisshaar, J. C. *J. Phys. Chem.* **1988**, *92*, 92. (b) van Koppen, P. A. M.; Bowers, M. T.; Beauchamp, J. L.; Dearden, D. V. In *Bonding Energetics in Organometallic Compounds*; Marks, T. J., Ed.; American Chemical Society: Washington, DC, 1990; p 34. (c) van Koppen, P. A. M.; Brodbelt-Lustig, J.; Bowers, M. T.; Dearden, D. V.; Beauchamp, J. L.; Fisher, E. R.; Armentrout, P. B. *J. Am. Chem. Soc.* **1990**, *112*, 5663; **1991**, *113*, 3569. (d) Schultz, R. H.; Armentrout, P. B. *Ibid.* **1991**, *113*, 729.

[44] Low, J. J.; Goddard, W. A., III. *J. Am. Chem. Soc.* **1984**, *106*, 8321. Saillard, J.-Y.; Hoffman, R. *Ibid.* **1984**, *106*, 2206. Ziegler, T.; Tschinke, C.; Fan, L.; Becke, A. D. *Ibid.* **1989**, *111*, 9177. Koga, N.; Morokuma, K. *Ibid.* **1993**, *115*, 6883.

Scheme 2

$$\mathrm{Cp^*Rh(CO)_2} \xrightarrow[\text{liq Kr}]{h\nu} \mathrm{I + CO}$$

$$\mathrm{II + Kr} \overset{K_{eq}}{\rightleftarrows} \mathrm{I} + \mathrm{C_6H_{12}} \xrightarrow{k_{2A}} \mathrm{III + Kr}$$

$$\mathrm{I} \xrightarrow{k_3} \text{products}$$

Scheme 3

$$\mathrm{I} \underset{k_s}{\overset{k_{-s}}{\rightleftarrows}} \mathrm{Cp^*Rh(CO) + Kr}$$

$$\mathrm{Cp^*Rh(CO) + C_6H_{12}} \xrightarrow{k_{ins}} \mathrm{III}$$

One final point relevant to the mechanism proposed above is that the barrier for interconversion of I and II must be much lower than that for the activation step that produces the final product, III. While the exact mechanism by which the alkane displaces the solvent is unknown, we propose that (as discussed above for the general case of ligand substitution at centers containing cyclopentadienyl-type ligands) it is an associative pathway. In our study of the substitution kinetics of Cp*Rh(CO)Xe + CO, we reported that $\Delta H^{\ddagger} = 2.4 \pm 0.3$ kcal/mol for the substitution, i.e. lower than both the C—H activation barrier we measure here, about 5 kcal/mol, and the probable Rh–Rg bond dissociation energy of about 5–10 kcal/mol, which indicates that an associative ligand exchange reaction is energetically favored over a dissociative one and that is consistent with the rest of the energetics we measure in this study. We therefore conclude that the mechanism shown in Scheme 1 is a reasonable explanation for our results not only because it is consistent with the observed kinetics but also because the intermediates proposed are themselves reasonably postulated to exist.

The mechanism given in Scheme 1 is kinetically indistinguishable from the similar preequilibrium mechanism given in Scheme 2. This mechanism, in which the solvated complex is in a "dead-end" equilibrium with a nonactivating σ-complex and alkane activation occurs in an independent bimolecular reaction, also predicts saturation kinetics as given in eq 3.

$$k_{obs} = \frac{k_{2A}[\mathrm{C_6H_{12}}][\mathrm{Kr}]}{K_{eq}[\mathrm{C_6H_{12}}] + [\mathrm{Kr}]} + \frac{k_3}{1 + (K_{eq}[\mathrm{C_6H_{12}}]/[\mathrm{Kr}])} \qquad (3)$$

While we cannot rule out the mechanism given by Scheme 2 on experimental grounds, we consider it to be unlikely for several reasons. First, it posits that there is some orientation of the alkane relative to the metal center from which activation cannot take place, but it is strongly enough bound that it cannot find the reactive orientation once the σ-complex is formed. While such a conformational dependence on reactivity might be remotely conceivable for cyclohexane, our observation of saturation kinetics in the related reaction of Cp*Rh(CO)$_2$ with the symmetrical molecule neopentane[33] indicates that this sequence is unlikely to be occurring. Furthermore, an Arrhenius analysis of the "k_{2A}" values derived by using eq 3 to model the concentration-dependent rates yields $A \approx 10^{13}$, which is considerably higher than the value that one would expect for a bimolecular reaction. In any case, if Scheme 2 were the actual mechanism, then the true values of k_{2A} would be about 100 times larger than those reported in Table 1 for k_2. The values of K_{eq}, however, are the same whether eq 2 or eq 3 is used to analyze the data.

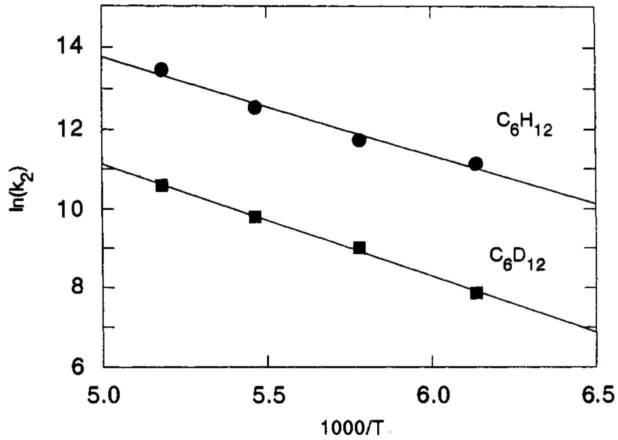

Figure 10. Arrhenius plots for activation of $\mathrm{C_6H_{12}}$ (circles) and $\mathrm{C_6D_{12}}$ (squares) by Cp*Rh(CO)$_2$ in liquid Kr. The solid lines are fits to the data with E_a = 4.6 kcal/mol, log A = 10.9 for $\mathrm{C_6H_{12}}$ and E_a = 5.8 kcal/mol, log A = 11.2 for $\mathrm{C_6D_{12}}$.

While we have postulated an associative mechanism for substitution by alkane at the solvated metal center I, a dissociative mechanism such as that shown in Scheme 3 also predicts saturation behavior at high alkane concentration. In this mechanism, the activation step involves a "naked" monocarbonyl species, Cp*Rh(CO). A steady-state analysis of this mechanism predicts that k_{obs} should be given by eq 4.

$$k_{obs} = \frac{k_{-s}k_{ins}[\mathrm{C_6H_{12}}]}{k_{ins}[\mathrm{C_6H_{12}}] + k_s[\mathrm{Kr}]} \qquad (4)$$

In this case, the limiting rate constant is predicted to be k_{-s}, the rate at which I dissociates to form the "naked" monocarbonyl. Although Scheme 3 does predict that only one intermediate should be observable, two pieces of evidence weigh heavily against the likelihood of this mechanism being correct. First, eq 4 predicts saturation only when $k_{ins}[\mathrm{C_6H_{12}}]$ dominates k_s[Kr]. Even at the highest cyclohexane concentrations used, [Kr] > 300[$\mathrm{C_6H_{12}}$], and so at saturation in this scheme k_{ins} must be on the order of 100–1000 times greater than k_s, the rate of reattachment of Kr to the monocarbonyl. Because k_s is almost certainly near the diffusion limit, it is difficult to believe that the intramolecular insertion rate is so much larger. A more serious objection to the mechanism in Scheme 3 is that it predicts a saturation rate constant k_{-s} that is *independent* of the nature of the alkane. The values for k_2 listed in Table 1 show that the saturation rate differs by 1 order of magnitude between $\mathrm{C_6H_{12}}$ and $\mathrm{C_6D_{12}}$. The saturation rate for C—H activation of neopentane under otherwise identical experimental conditions is different from either of these.[20a,33] We thus rule out the mechanism shown in Scheme 3 as a plausible explanation for our observations.

Another possible explanation for the observed saturation behavior is that as more alkane is added to the reaction mixture, the alkane molecules aggregate rather then remain as individual, solvent-separated molecules. If this were the case, the integrated FTIR absorbances would still be linearly related to the number of alkane molecules present in the cell, but would not reflect accurately the frequency with which the rhodium intermediate encounters an alkane molecule. Under these circumstances, the probability of a reactive encounter would be just the probability of encountering one of these aggregates and reacting with a molecule at its surface, and hence might no longer be proportional to the alkane "concentration" as measured by FTIR. There are numerous problems with this interpretation as well. First, the FTIR spectra themselves are not consistent with large numbers of aggregates, which when present appear as broad lines in the spectrum,[45] as opposed to the sharp peaks (fwhm ≤ 4 cm^{-1}) we

---

(45) Beattie, W. H.; Maier, W. B., II; Freund, S. M.; Holland, R. F. *J. Phys. Chem.* **1982**, *86*, 4351. Schauer, M. W.; Lee, J.; Bernstein, E. R. *J. Chem. Phys.* **1982**, *76*, 1982. Kyle, K. R.; Bergman, R. G.; Moore, C. B. Unpublished results.

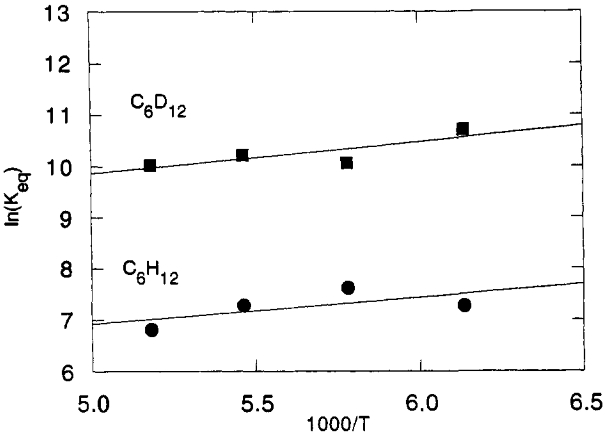

Figure 11. Van't Hoff plots for the preequilibrium constants K_{eq} between Cp*Rh(CO)···Kr and Cp*Rh(CO)···alkane for the alkane = C_6H_{12} (circles) and C_6D_{12} (squares). The solid lines are fits to the data with $\Delta H = -1.6$ kcal/mol, $\Delta S = 6.0$ eu for C_6H_{12} and $\Delta H = -1.6$ kcal/mol, $\Delta S = 11.6$ eu for C_6D_{12}.

invariably observe here. Furthermore, it seems unlikely that the deviations from linearity would occur at such different "concentrations" for C_6H_{12} and C_6H_{12}, but be so similar in general between cyclohexane and neopentane.[33]

2. Activation and Equilibrium Parameters from the Temperature-Dependent Kinetics. Assuming the mechanism outlined in Scheme 1, we can use the temperature-dependent kinetic data shown in Table 1 to calculate activation parameters. Figure 10 is an Arrhenius plot for k_2, the intramolecular activation step. The preexponential factor for both C_6H_{12} and C_6D_{12} is approximately 10^{11}, consistent with the intramolecular activation step we propose in Scheme 1, lending further support to our proposed mechanism. Eyring analyses of the temperature dependences of k_2 yield $\Delta H^{\ddagger} = 4.2 \pm 0.5$ kcal/mol, $\Delta S^{\ddagger} = -9.9 \pm 1.4$ eu for C_6H_{12} and $\Delta H^{\ddagger} = 5.3 \pm 0.5$ kcal/mol, $\Delta S^{\ddagger} = -9.0 \pm 1.2$ eu for C_6D_{12}. These values are similar to those proposed in earlier experimental[4b,46] and theoretical[44] studies of alkane C—H activation at group 9 metal centers. The negative $\Delta S^{\ddagger}$ observed in both cases is further evidence for intramolecular activation in the transition state.

We can derive the thermodynamics of the preequilibrium from the variation of K_{eq} with temperature. These quantities will necessarily be less accurate than those derived from k_2, as the individual values of K_{eq} are determined from the rising portion of the saturation curve, where small errors in the measured alkane concentration have a significant effect. Nonetheless, the van't Hoff plots shown in Figure 11 are linear and consistent with a preequilibrium in which the alkane complex **II** lies lower in energy than the krypton complex **I**. We derived $\Delta H = -1.6 \pm 0.4$ kcal/mol for *both* C_6H_{12} and C_6D_{12}, and $\Delta S = +6.0$ eu for the former and +11.6 eu for the latter.

The above information enables us to construct the reaction coordinate energy diagram shown for reaction at 183 K in Figure 12. In the following section, we discuss the differences in the behavior of cyclohexane-d_0 and -d_{12} that this diagram reveals.

3. Isotope Effects on the Kinetics and Thermodynamics. The activation of cyclohexane in krypton proceeds considerably more slowly for C_6D_{12} than it does for C_6H_{12}, as Figure 5 and Table 1 clearly show. The large isotope effect on k_2 (approximately a factor of 10–20 over the temperature range studied) is straightforwardly explained. Since the zero-point energy of a C–D bond is lower than that for an equivalent C—H bond by 1.2 kcal/mol,[47] it is not surprising that the cleavage step is quite sensitive to the hydrogen isotope involved. The difference in the energies of activation ($\Delta\Delta G \approx 1$ kcal/mol) for the two isotopomers is completely consistent with this zero-point energy difference. Further, the small difference in $\Delta S^{\ddagger}$ is quite sensible, as we would not expect there to be much difference in the entropy of activation between two such similar transition states.

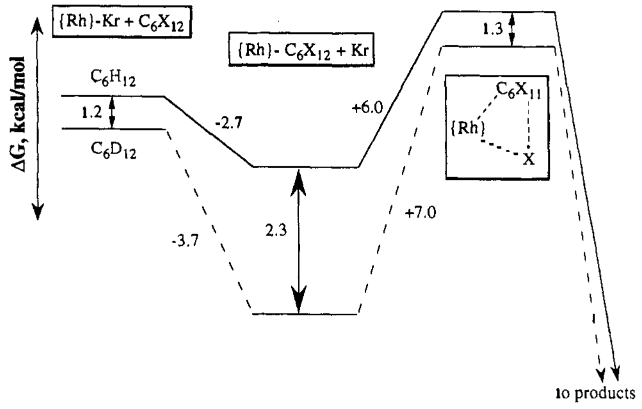

Figure 12. Reaction coordinate free energy diagram for activation of C_6H_{12} and C_6D_{12} by Cp*Rh(CO)$_2$ in liquid Kr at 183 K. The reaction coordinate is assumed to be the C—H or C—D bond being activated, and relative ΔG values for the intermediates are from the values of K_{eq} given in Table 1 and $\Delta H^{\ddagger}$ and $\Delta S^{\ddagger}$ given in the text.

As mentioned above, k_{obs} reaches its saturation value at a much lower concentration of C_6D_{12} than it does for C_6H_{12}. Since the rate at which k_{obs} approaches saturation as a function of alkane concentration depends on K_{eq} (eq 2), this is equivalent to saying that $K_{eq}(C_6D_{12}) \gg K_{eq}(C_6H_{12})$, and indeed, as shown in Table 1, K_{eq} is approximately 20 times greater for activation of C_6D_{12} than it is for C_6H_{12}. As shown in Figure 12, at 183 K, this is equivalent to saying that the $\Delta\Delta G$ *increases* from 1.2 to 2.3 kcal/mol; that is, C_6D_{12} must bind more strongly to the rhodium center than C_6H_{12} does. Although our van't Hoff derivation indicates that ΔH is similar (within rather large error bars) for binding the two isotopomers, the quantity of interest for understanding the isotope effect is ΔG, i.e. the binding constant, which in this case clearly favors complexation of the perdeuterated alkane. And while the quantitative measures of the binding constant and the exact amount to which it can be divided into enthalpic and entropic portions are uncertain, the *qualitative* observation is clear.

This unusual *inverse* equilibrium isotope effect is much more difficult to explain than the normal isotope effect on the activation step. The same zero-point energy effects that led to the large normal isotope effect on k_2 ought to lead to a normal isotope effect on the relative binding propensity of the σ-bound alkane complex. Such an effect is seen, for example, in the compound $HOs_3(CO)_{10}CH_nD_{3-n}$ (n = 1 or 2). In this compound, there is an agostic interaction between one of the Os atoms and one of the hydrogen atoms of the methyl group. This agostic site is preferentially occupied by an H rather than a D atom.[48]

Unfortunately, we cannot unambiguously determine which of the conceivable secondary effects is the most important one for the present system. It seems that there are two most likely possibilities. It could be that there are significant differences in the entropies of solvation for the metal interacting with either C_6H_{12} or C_6D_{12}. The van't Hoff plots shown in Figure 11 indicate that this may be an important factor, as we determine ΔS for replacing the Kr with C_6D_{12} to be about twice that for replacing it with C_6H_{12}. Unfortunately, as discussed above, the absolute errors in our determination of ΔH and ΔS are sufficiently large that we cannot state unequivocally that the difference in alkane binding is primarily an entropic effect. A second possibility for explaining the greater relative binding propensity of C_6D_{12} is that vibrational modes other than the C—H (C—D) stretch of the bond being broken make significant contributions to the overall zero-point energy of the metal–alkane complex. Certainly, we

---

(46) Stoutland, P. O.; Bergman, R. G.; Nolan, S. P.; Hoff, C. D. *Polyhedron* **1988**, *7*, 1429.

(47) Calculated from C—H and C—D vibrational frequencies for C_6H_{12} and C_6D_{12} given in the following: Sverdlov, L. M.; Kovner, M. A.; Krainov, E. P. *Vibrational Spectra of Polyatomic Molecules*; Wiley: New York, 1974.

(48) Calvert, R. B.; Shapley, J. R. *J. Am. Chem. Soc.* **1978**, *100*, 7726.

would expect the hindered rotations of the alkane to be lower in frequency for the perdeuterated alkane than for the perprotiated one, and it could be these low-frequency modes that contribute to the zero-point energy differences of the complexes. Unfortuantely, while this conjecture seems reasonable, we cannot measure the frequencies and relative intensities of these modes in intermediate **II** using our apparatus.

A recent *ab initio* calculation[49] of equilibrium deuterium isotope effects for oxidative addition of various isotopomers of CH_4 to *trans*-$Ir(PR_3)_2(CO)X$ (X = Cl or CH_3) predicts a normal equilibrium isotope effect on the addition, which is consistent with our observation of a normal isotope effect on k_2. More important, however, is the prediction of the calculation that the "vibrational excitation" contribution to the isotope effect should be strongly inverse due to the presence of low-energy bending vibrations present in the methyl complex but not in free methane. While the calculations were done on a somewhat different system and for room-temperature reactants, the conclusions of that study do tie in neatly with the suggestions we have posited for the present system.[50]

4. Photolysis in Xe: Additional Confirmation of the Reaction Mechanism. One reason why accurate determination of the equilibrium isotope effect is so difficult is that, in liquid Kr, K_{eq} is so large. Thus, since [Kr] is about 20 M,[31] $[Kr]/K_{eq}$ is on the order of 10^{-2}, i.e. comparable or even larger than typical alkane concentrations. It was with this consideration in mind that we performed a series of photolysis experiments in liquid Xe. We expect that, since Xe binds more strongly than Kr to Rh,[12] K_{eq} (Scheme 1) should be much smaller when Xe is the solvent than when Kr is. If K_{eq} is sufficiently small, then $[Xe]/K_{eq} \gg [\text{alkane}]$, and eq 2 reduces to

$$k_{obs} = \frac{k_2 K_{eq}[C_6H_{12}]}{[Xe]} + k_3 \qquad (5)$$

Since in Xe, k_3 is on the order of 1 s^{-1} (ref 12), i.e. much smaller than the uncertainties in our rate measurements, it is not explicitly considered any further in our analysis.[51] Thus, the mechanism of Scheme 1 predicts that, in Xe, k_{obs} should *not* show saturation behavior, but rather be linear in alkane concentration. Furthermore, since in Kr the normal isotope effect on k_2 is very nearly the same absolute magnitude as the inverse isotope effect on K_{eq}, these two effects should cancel when Xe is used as the solvent, so there should not be any significant isotope effect on k_{obs}. As Figures 8 and 9 show, there is indeed no obvious saturation even at $[C_6H_{12}]$ = 0.15 M, and a much smaller isotope effect on k_{obs}. Since k_{obs} is simply a linear function of alkane concentration, it is not possible to determine k_2 and K_{eq} independently for reaction in Xe. If we assume, however, that the intramolecular rate constant k_2 is solvent-independent,[52] then we can derive K_{eq} in Xe from eq 5 by extrapolating the values of k_2 measured in Kr to the temperatures at which we performed the Xe experiments and using that value for k_2 along with the literature value of the density of liquid Xe.[53] In Figure 13, we show a "pseudo-van't Hoff" plot from these values of K_{eq}, from which we can derive ΔH = 1.5 ± 0.5 kcal/mol, ΔS = 0.2 ± 2.2 eu for C_6H_{12} and ΔH = −0.7 ± 0.6 kcal/mol, ΔS = −4.6 ± 2.8 eu for C_6D_{12}. In Xe, for both C_6H_{12} and C_6D_{12}, K_{eq} is less than 1, and the overall energetics of the equilibrium are approximately thermoneutral for both isotopomers. Nonetheless, just as in Kr, in Xe, K_{eq} is approximately 1 order of magnitude larger for C_6D_{12} than it is for C_6H_{12}. Thus, our results for photolytic activation of cyclohexane-d_0 and -d_{12} by $Cp^*Rh(CO)_2$ in liquid Xe are consistent with, and hence support, the overall mechanism derived for the analogous reaction in liquid Kr and shown in Scheme 1.

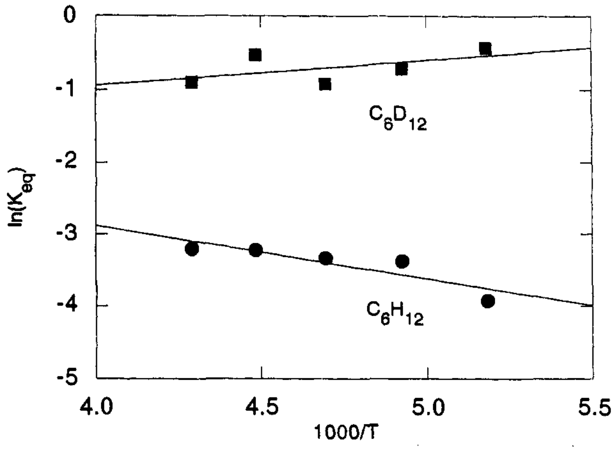

Figure 13. Van't Hoff plot for activation of C_6H_{12} (circles) and C_6D_{12} (squares) by $Cp^*Rh(CO)_2$ in liquid Xe. See text for explanation of how K_{eq} is derived in these systems. The solid lines are fits to the data with ΔH = 1.5 kcal/mol, ΔS = 0.2 eu for C_6H_{12} and ΔH = −0.7 kcal/mol, ΔS = −4.6 eu for C_6D_{12}.

Conclusions

Photolysis of $Cp^*Rh(CO)_2$ in liquid Kr or Xe yields a solvated monocarbonyl intermediate. In the presence of cyclohexane, this intermediate reacts to form an activated product in which the metal atom inserts into an alkane C—H bond to form a rhodium alkyl hydride species. In Kr, the reaction rate measured as a function as alkane concentration rises to a saturation value. We interpret this behavior in terms of a preequilibrium model in which the solvated intermediate is initially in equilibrium with a weakly bound metal–alkane complex. This latter species then undergoes intramolecular C—H activation to form the alkyl hydride product. We measure the ΔH^* for this activation step to be 4.2 ± 0.5 kcal/mol for C_6H_{12} and 5.3 ± 0.5 kcal/mol for C_6D_{12}. This difference in activation energies is indicative of a large deuterium isotope effect on the activation step. We also observe an unusual *inverse* isotope effect in the preequilibrium in which K_{eq} for formation of the alkane complex is 1 order of magnitude larger for C_6D_{12} than it is for C_6H_{12}. Although analogous reactions carried out in liquid Xe do not show saturation behavior due to much lower values of K_{eq}, the inverse isotope effect on the equilibrium persists and is of the same magnitude as it is in liquid Kr.

Acknowledgment. This work was supported by the Director, Office of Energy Research, Office of Basic Energy Sciences, Chemical Sciences Division, of the U.S. Department of Energy under Contract No. DE-AC03-76SF00098. We would also like to thank Johnson Matthey Aesar/Alfa for a generous gift of rhodium chloride through its precious metals loan program, and Dr. B. R. Bender (ColoradoState University) for disclosure of results prior to publication .

---

(49) Abu-Hasanayn, F.; Krogh-Jespersen, K.; Goldman, A. S. *J. Am. Chem. Soc.* **1993**, *115*, 8019.

(50) **Note added in proof**: Two recent studies report hydrocarbon–metal binding and/or activation isotope effects that are relevant to our observations: (a) the measurement of intra- vs intermolecular isotope effects on methane activation in early transition metal systems by Schaller, C. P.; Bonanno, J. B.; Wolczanski, P. T. *J. Am. Chem. Soc.* **1994**, *116*, 4133; (b) the determination of an inverse isotope effect on the binding of C_2D_4 to a $Os_2(CO)_8$ fragment by Bender, B. R.; Norton, J. R., unpublished results.

(51) The linear fits to Figures 8 and 9 have nonzero intercepts. Part of this is due to the time constant of the digital oscilloscope as discussed above,[29] but there also seems to be a temperature-dependent part of the nonzero intercept which implies a significantly shorter lifetime for $Cp^*Rh(CO)Xe$ than our previous study reported.[12] As the current analysis depends only on the slope of the linear fit, this discrepancy was not investigated further.

(52) We can make a less restrictive assumption instead, namely, that the *relative* values of k_2 for C_6H_{12} and C_6D_{12} (i.e. the magnitude of the isotope effect) are solvent-independent, but this assumption would not affect our determination of the relative values of K_{eq}.

(53) Terry, M. J.; Lynch, J. T.; Bunclark, M.; Mansell, K. R.; Staveley, L. A. K. *J. Chem. Thermodyn.* **1969**, *1*, 413.